Frequency dependence of thermal noise in gram-scale cantilever flexures

Thanh T-H. Nguyen,[1] Conor M. Mow-Lowry,[2] Bram J. J. Slagmolen,[1] John Miller,[3] Adam J. Mullavey,[4] Stefan Goßler,[5] Paul A. Altin,[1,*] Daniel A. Shaddock,[1] and David E. McClelland[1]

[1]*Centre for Gravitational Physics, The Australian National University, Science Rd 38a,*
2601 Canberra, ACT, Australia
[2]*School of Physics and Astronomy, The University of Birmingham, Edgbaston,*
Birmingham B15 2TT, United Kingdom
[3]*LIGO Laboratory, Massachusetts Institute of Technology, Cambridge, Massachusetts 02139, USA*
[4]*LIGO Laboratory, Ligo Rd, Livingston, Louisiana 70754, USA*
[5]*Albert-Einstein-Institut, Max-Planck-Institut für Gravitationsphysik, D-30167 Hannover, Germany*

We present measurements of the frequency dependence of thermal noise in aluminum and niobium flexures. Our measurements cover the audio-frequency band from 10 Hz to 10 kHz, which is of particular relevance to ground-based interferometric gravitational wave detectors, and span up to an order of magnitude above and below the fundamental flexure resonances. Results from two flexures are well explained by a simple model in which both structural and thermoelastic loss play a role. The ability of such a model to explain this interplay is important for investigations of quantum-radiation-pressure noise and the standard quantum limit. Furthermore, measurements on a third flexure provide evidence that surface damage can affect the frequency dependence of thermal noise in addition to reducing the quality factor, a result which will aid the understanding of how aging effects impact on thermal noise behavior.

I. INTRODUCTION

Thermal fluctuations have become one of the fundamental sources of noise in high-precision experiments and are of increasing interest to many research groups [1–5]. A prime example is interferometric gravitational wave (GW) observatories [6–8], in which the mitigation of thermal noise in the audio-frequency band from 10 Hz to 10 kHz constitutes one of the most challenging aspects of the design of mirrors and suspension systems [9–11]. In particular, as GW observatories are required to operate continuously for months or even years, understanding how the thermal noise spectrum can change over time is important, especially in light of recent reports from the VIRGO experiment of surface damage on the blade springs which form the basis of that interferometer's suspension system [12]. It is also crucial to understand the role of thermal noise in experiments investigating quantum-radiation-pressure noise (QRPN) and the standard quantum limit (SQL) [13]. When dominated by structural damping [14], thermal noise above the mechanical resonance rolls off with frequency faster than QRPN, so that at sufficiently high frequencies the SQL can be observed. However, thermal noise when dominated by viscous damping exhibits the same frequency dependence as QRPN, making it necessary to cool such a system (typically to below 1 K) in order to observe the SQL.

Here, we present direct measurements of broadband displacement spectra which are limited by thermal noise across the audio-frequency band (spanning over a decade above and below the fundamental flexure resonances). The oscillator is a cantilever flexure with an effective mass on the scale of ∼1 g. Cantilever flexures are used in a wide range of opto-mechanical experiments [2,5,15,16] and feature in designs for mirror suspension systems in future gravitational wave detectors [17,18]. We use cavity readout and Pound-Drever-Hall (PDH) locking [19] to retrieve the flexure displacement, allowing us to observe fluctuations below 10^{-16} m$\sqrt{\text{Hz}}$.

Our experiment has the ability to resolve different frequency dependences of thermal noise in the audio-frequency band. Our analysis indicates that, for two of our flexures, structural noise dominates the displacement fluctuation spectra at low frequencies, whereas thermoelastic noise dominates at higher frequencies, until frequency noise compromises the measurement. Previous measurements have been reported showing coating and mirror thermal noise as the dominant source of fluctuations in various regions of the displacement spectrum [20–23]. Our flexure resonances fall in the intermediate region where structural and thermoelastic loss have comparable magnitudes. While structural and viscous damping have been studied before [24–26], to our knowledge no experiments to date have explored this crossover regime. Our results are well explained by a simple model which includes both effects. This agreement confirms the frequency dependence of these different thermal noise mechanisms, which is vital for experiments seeking to measure QRPN and the SQL, especially in the case of niobium which, with

*paul.altin@anu.edu.au

its low bulk loss, is a material of interest for such experiments. Furthermore, we present measurements from a second niobium flexure with visible surface damage for which the thermal noise is not explained by the same model, unless an extra viscous damping is included. This indicates that surface damage can change the frequency dependence of thermal noise in addition to reducing an oscillator's quality factor, which will be an important consideration for taking account of aging in GW detector suspension systems.

II. EXPERIMENTAL SYSTEM

Monolithic inverted-pendulum flexures [Fig. 1(b)] were manufactured from aluminum (1100 alloy) and niobium by electric discharge machining [27]. The niobium flexures were annealed in vacuum and chemically etched to obtain a high Q factor [28]. The geometrical simplicity of the mechanical oscillators was intended to isolate the fundamental resonant frequencies from higher-order modes.

The aluminum flexure membrane was 5 mm wide, 1 mm high, and 120 μm thick. A mirror 1/4 in. in diameter and 2 mm thick was glued to the top of the flexure. The effective mass of the flexure (including the mirror) was 0.4 g, resulting in a fundamental resonance of 271 Hz. The quality factor at this resonance was independently determined from a ringdown measurement to be $Q = 2200$.

The first niobium flexure membrane was 6.35 mm wide, 1 mm high, and 72 μm thick. A dielectric mirror 7 mm in diameter and 1 mm thick was glued to the top of the flexure structure. With an effective mass of 0.7 g, the fundamental resonant frequency is at 85 Hz with $Q = 44000$, also independently determined using a ringdown measurement.

A second niobium flexure with a 6.35×1.0 mm, 200 μm thick membrane was also manufactured, with a resonant frequency of 302 Hz and a quality factor of

$Q = 1540$, measured by ringdown and confirmed by a direct measurement of the mechanical transfer function.

To measure the extremely small thermal displacements with a high signal-to-noise ratio, a flexure is placed into a vacuum chamber and acts as the back mirror of a Fabry-Perot test cavity (TC). Displacements of the flexure imprint a phase shift onto the light bouncing off the mirror, which is amplified by approximately a factor of the cavity finesse. The layout of the experiment is shown in Fig. 1(a). The TC was 12 mm long and comprised a front mirror glued to a piezoelectric transducer (PZT) [29] in addition to the back mirror on the flexure. The cavity finesse was 600 and 700 for the aluminum and niobium flexure experiments, respectively. The TC was kept on resonance using the PDH locking technique [19,30], and fluctuations in the cavity length were read out via the error signal of the PDH lock (labelled "Readout" in Fig. 1), corrected using the measured closed-loop servo response.

To successfully measure thermal fluctuations using this technique, noise on the frequency of the interrogating laser must be reduced to below the equivalent thermal noise displacement, since these would otherwise appear as changes in the cavity length. To achieve this, the laser was locked to a high-finesse ($\mathcal{F} = 6000$), 20-cm-long Zerodur reference cavity suspended in vacuum [27]. It is also critically important that thermal fluctuations be the dominant source of changes in the cavity length. For this, the TC is suspended inside the vacuum chamber by a multistage vibration isolation system [31], which provides an effective "seismic wall" at 10–40 Hz.

III. DISPLACEMENT NOISE MEASUREMENTS

The measured displacement fluctuation spectra for the three flexures are shown in Fig. 2. Also shown on these plots are the laser frequency noise, converted to an equivalent displacement noise, and electronic readout noise, as well as the expected thermal noise of the mirror coatings and PZT [32,33]. The measured displacement spectra are above all of these noise sources, and therefore expected to be dominated by thermal fluctuations, up to an order of magnitude above and below the fundamental mechanical resonances. Laser frequency noise begins to dominate the spectra at around 5–10 kHz. Calibration lines were injected into each spectrum, setting an experimental uncertainty on the displacement of approximately 20%.

IV. THERMAL NOISE MODEL

Thermal noise is present in all macroscopic oscillating systems, driven by the thermal energy $k_B T$ present in every degree of freedom. From the fluctuation-dissipation theorem, the power spectrum of the thermal fluctuations $x_{\text{th}}(t)$ in a harmonic oscillator at temperature T can be determined from its mechanical response, characterized by oscillation frequencies ω_k, their effective masses m_k, and corresponding
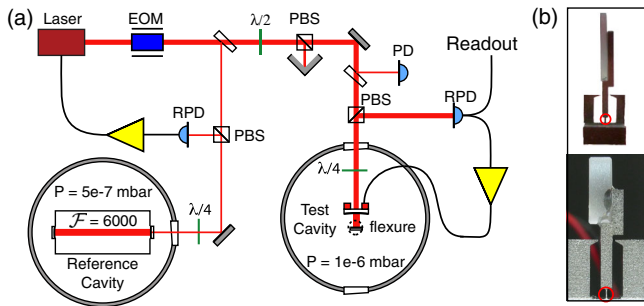

FIG. 1 (color online). Schematic of the experimental setup (PBS: polarising beam splitter, EOM: electro-optic modulator, PD: photodiode monitoring input power, RPD: photodiode measuring reflected power). The insets A and B show the rear mirror of the test cavity mounted on the niobium and aluminum flexures (red circles). Not shown are two steering mirrors inside the vacuum; the $\lambda/4$ plate is placed directly in front of the test cavity to ensure that the polarization on these mirrors is linear.
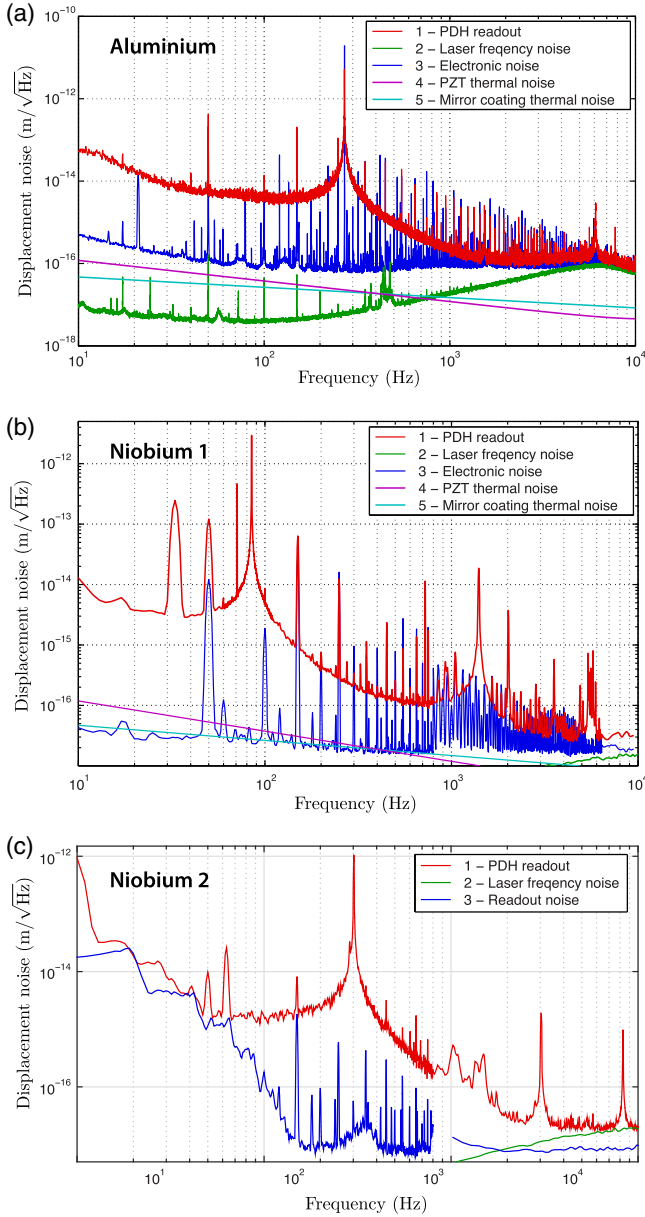
FIG. 2 (color online).   Measured displacement noise spectra for the aluminum (a) and niobium (b,c) flexures. Readout and laser frequency noise are also shown as indicated in the legends. The spectra are clear of other noise sources on either side of the fundamental resonant frequencies.

losses $\phi_k(\omega)$, which are generally frequency dependent [14,34]. The equation describing this power spectrum is

$$\hat{X}^2_{\text{th}}(\omega) = \sum_{k=0}^{n} \frac{4k_B T \omega_k^2 \phi_k(\omega)}{m_k \omega [(\omega_k^2 - \omega^2)^2 + \omega_k^4 \phi_k^2(\omega)]}, \quad (1)$$

where k_B is the Boltzmann constant. Here, the dimensionless loss parameter $\phi_k(\omega)$ represents the linear sum of all losses in the system for the kth mode; its value on resonance

determines the quality factor of that resonance as $\phi_k(\omega_0) = 1/Q_k$.

Our model takes into account damping of all relevant mechanical modes by a combination of structural loss ϕ_{struc}, due to internal friction, and viscous thermoelastic loss $\phi_{te,k}(\omega)$, caused by heat flow as different parts of the material are subjected to differential stresses. The total loss for a particular mode is taken to be

$$\phi_k(\omega) = \phi_{\text{struc}} + \phi_{te,k}(\omega), \quad (2)$$

which should match the value obtained from ringdown measurements. The structural loss is the same for all modes and is independent of frequency [14]; in the absence of any other loss mechanisms, the inverse of the structural loss alone would determine the quality factor Q of the oscillator. On the other hand, thermoelastic loss varies with frequency and is dependent on the bulk material and geometry of the flexure. It can also be different for different oscillation modes.

In general, the thermoelastic loss of a mode k is described in terms of a strength Δ and characteristic time τ_k [35], as

$$\phi_{te,k}(\omega) = \Delta \frac{\omega \tau_k}{1 + (\omega \tau_k)^2}, \quad (3)$$

where

$$\Delta = \frac{\alpha^2 E_y T}{\rho C_v}, \qquad \tau_k = \frac{\rho C_v l_k^2}{\kappa \pi^2}. \quad (4)$$

In these equations, α, E_y, ρ, C_v, and κ represent the linear thermal expansion coefficient, Young's modulus, density, specific heat, and thermal conductivity of the flexure material, respectively. Values for these are given in Table I. The parameter l_k represents the path length along which heat flows as the material experiences stress and strain. This varies depending on the mode of oscillation; for example, the path length l_0 for the fundamental (bending)

TABLE I.   Thermal noise model parameters.

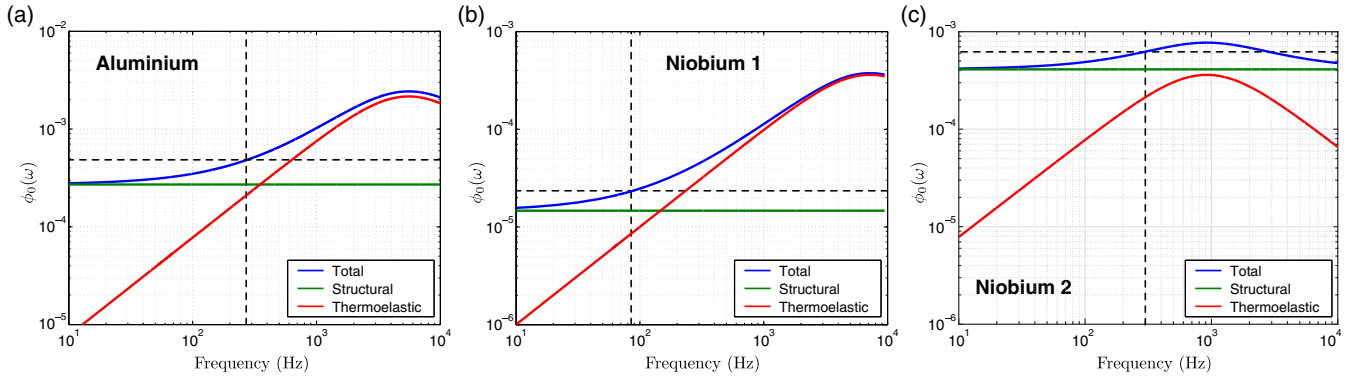| Parameters	Aluminum	Niobium	Units
Resonant frequency	271	85/302	Hz
Mirror diameter	6.35×10^{-3}	6.35×10^{-3}	m
Mirror thickness	2×10^{-3}	1×10^{-3}	m
Young's modulus E_y	71	105	GPa
Linear expansion coefficient α	23×10^{-6}	7.3×10^{-6}	K^{-1}
Specific heat C_v	904	265	J(kgK)$^{-1}$
Thermal conductivity κ	138	54	W(mK)$^{-1}$
Density ρ	2820	8578	kgm^{-3}
Thermoelastic resonance f_{te}	5.6×10^3	7.2×10^3	Hz

FIG. 3 (color online). Calculated frequency-dependent loss $\phi_0(\omega)$ for the fundamental oscillation mode of the aluminum (a) and niobium (b,c) flexures, showing the contributions of structural ϕ_{struc} and thermoelastic $\phi_{te,0}(\omega)$ damping. The fundamental flexure resonance frequency for each material is indicated by the vertical dashed line, and the total loss determined from the measured quality factor is marked by the horizontal line.

mode of our cantilever flexures is simply the membrane thickness, while for a higher-order shear mode l_k could depend additionally on the width and height of the membrane. The characteristic time taken for heat to be transferred across this distance is given by τ_k and gives rise to a peak in the frequency response at $\omega_k = 1/\tau_k$.

Figure 3 shows the predicted frequency-dependent loss, made up of structural and thermoelastic components, for our three flexures in the frequency range of interest. The fundamental resonant frequencies are indicated by vertical dashed lines, and the total loss calculated from the measured quality factor is shown as a horizontal line. Equations (2) and (3) then allow us to infer the structural loss for each flexure. The values obtained in this way are summarized in Table II. The inferred structural loss values for the aluminum and first niobium flexure are consistent with those reported in other work [28].

Our model predicts much higher thermoelastic loss at the fundamental resonance for the second niobium flexure due to its increased thickness, which shifts the thermoelastic peak to lower frequencies according to Eq. (4). This is consistent with the significantly lower quality factor. However, the inferred structural loss for this flexure is also much higher than for the first niobium flexure, which is unexpected since the two flexures are made of the same material.

Other loss mechanisms were also investigated, including damping from residual background gas collisions, loss

TABLE II. Loss coefficients $\phi_0(\omega_0)$ from the thermal noise model at the fundamental resonance frequency of each flexure. The uncertainty in these coefficients is dominated by the displacement calibration uncertainty of 20%.

Flexure	Aluminum	Niobium 1	Niobium 2
ϕ_{tot} (measured)	4.8×10^{-4}	2.3×10^{-5}	6.2×10^{-4}
ϕ_{te} (from model)	2.1×10^{-4}	8.5×10^{-6}	2.1×10^{-4}
ϕ_{struc} (inferred)	2.7×10^{-4}	1.5×10^{-5}	4.1×10^{-4}

from the flexure clamping, and the amount and type of glue used (initially "Vac-Seal," a vacuum compatible two-part epoxy, and subsequently superglue). None of these tests showed significant changes to the off-resonant thermal noise.

V. COMPARISON AND DISCUSSION

We now compare the predictions of the model developed above with our measured thermal noise displacement spectra.

Figure 4 shows the measured displacement noise spectra of the aluminum and high-Q niobium flexures overlaid with the thermal noise model developed above (Eq. (3) added in quadrature with the experimental noise sources discussed in Sec. III. No fitting was performed, and the ratio of the experimental and theoretical traces is also given for the purposes of comparison. For the aluminum flexure, the measured displacement deviates from the predicted total noise below 50 Hz, which is due to residual seismic coupling into the final test cavity suspension stage and spurious scattering of light onto the reflection photodiode. The niobium measurement follows the predicted noise trace well from 10 Hz up to 2 kHz.

In both of these cases, structural loss is the dominant noise source at frequencies below the fundamental resonance, while at higher frequencies the loss is dominated by thermoelastic damping. This feature is particularly noteworthy for QRPN experiments due to the different frequency dependence of these loss mechanisms [13]. Thermal noise originating from structural loss exhibits a $1/f^{2.5}$ rolloff, so that radiation pressure noise, which rolls off as $1/f^2$, can dominate at high frequencies. On the other hand, fluctuations due to thermoelastic loss have the same $1/f^2$ frequency dependence as radiation pressure and can therefore mask QRPN unless the system is cooled to cryogenic temperatures. As previously noted [11], one could tailor the flexure geometry to shift the thermoelastic peak out of the frequency band of interest, ensuring that
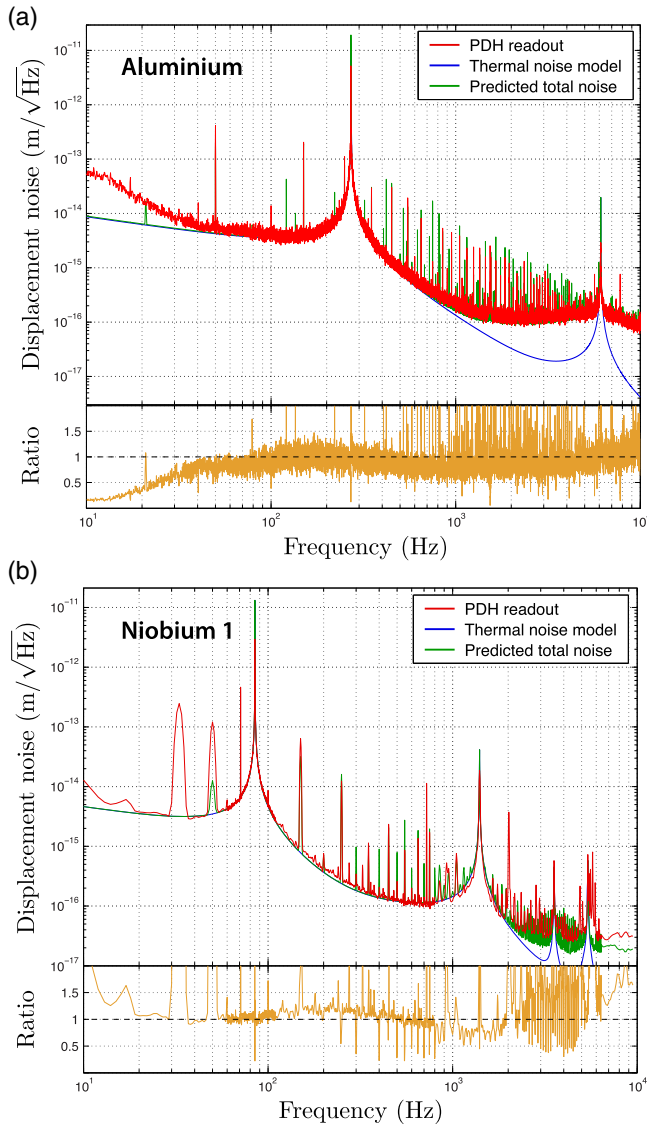
(a)

(b)

FIG. 4 (color online). Comparison of thermal noise measurement and model predictions for the aluminum and high-Q niobium flexures. The traces show the PDH error signal readout (red), the sum of structural and thermoelastic noise as predicted by the model detailed in Sec. IV (blue), and the quadrature sum of the thermal noise model and other experimental noise contributions (green). The lower plots show the ratio between the measured PDH error signal and the predicted total noise, which in both cases is close to unity between 50 and 5 kHz.

(a)

(b)

FIG. 5 (color online). Thermal noise of the low-Q niobium flexure. (a) Comparison of thermal noise models with the experimental data. Model (i) incorporates thermoelastic and structural damping as described in Sec. IV. Model (ii) uses the structural loss from the high-Q niobium flexure and the calculated thermoelastic loss, attributing the remaining damping to a viscous process. (b) Microscope image of a defect in the low-Q niobium flexure. The thin black line, circled in red, appears to be a crack running along one edge of the membrane.

QRPN will dominate the fluctuation spectrum. The simple model presented above, which fits the measured data well with no free parameters, could be used in the design of such experiments.

Figure 5(a) compares our thermal noise model with the experimental data for the second, low-Q niobium flexure. As noted in Sec. IV, our model predicts an unexpectedly high structural loss for this flexure, based on the measured quality factor. We now see that the model also predicts a qualitatively different frequency dependence to that
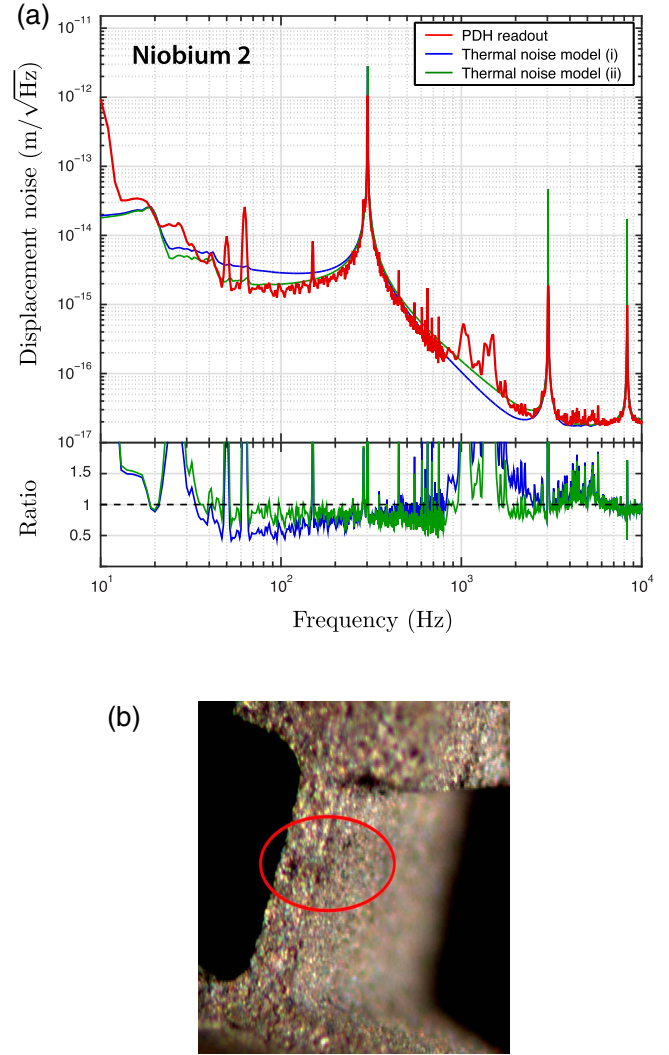
observed, particularly evident in the slope of the ratio between the model and the experimental data. This indicates that this flexure is not dominated by structural damping as predicted by the model. On the other hand, if we were to assume a similar structural loss to the first niobium flexure, the model developed in Sec. IV would predict a quality factor of $Q \sim 5000$, which is inconsistent with ringdown and transfer function measurements.

This discrepancy can be explained by a defect in the flexing membrane, visible under a microscope [Fig. 5(b)], which appears to run along one edge of the membrane. Such a defect could well introduce an additional source of

viscous damping due to rubbing [36], although this has not been investigated extensively. Trace (ii) in Fig. 5(a) shows a model with total loss determined by the measured quality factor $Q = 1540$, the same structural loss angle as for the first niobium flexure, thermoelastic loss calculated from Eq. (3), and the remainder attributed to an additional viscous damping. This model shows good agreement with the data, including below the fundamental resonance where the first model fails. From the low quality factor, the thermal noise spectrum, and the visible evidence of a defect in the flexure membrane, we therefore conclude that the flexure was damaged during fabrication or experimental usage and that the resulting crack not only reduced the quality factor but also added an additional source of viscous damping.

That a microscopic surface defect can change the frequency dependence of thermal noise is an important consideration, especially for GW observatories, which rely on knowledge of the frequency dependence of thermal noise over the lifetime of the instrument. Recently, the VIRGO Collaboration reported evidence of surface damage on the blade springs which form the basis of that interferometer's suspension system, even before the blades reach the breaking point [12]. A thermal noise spectrum which is dominated by viscous damping falls off more slowly with frequency (by a factor of $f^{1/2}$) than one dominated by structural noise. If an aging flexure develops surface cracks resulting in viscous damping and this effect is not taken into account, the thermal noise above the resonance may be significantly underestimated.

VI. CONCLUSIONS

We have reported measurements of off-resonance thermal noise for aluminum and niobium cantilever flexures in the audio-frequency band between 10 Hz and 10 kHz, using cavity readout and PDH locking to observe the displacement of the flexures due to thermal fluctuations at room temperature. Our experimental results show good agreement with a simple model which includes structural damping and frequency-dependent thermoelastic damping. Results from a third flexure with visible surface damage show a qualitatively different thermal noise spectrum which can only be explained using an additional viscous damping, demonstrating that surface damage can change the frequency dependence of thermal noise in addition to reducing the quality factor. These results are of particular interest for the design of suspension systems for next-generation gravitational wave observatories, as well as the understanding of aging effects in existing detectors. They also indicate that an appropriate choice of physical parameters should allow structural damping to dominate thermal noise well above the mechanical resonance, an important requirement in designing an experiment to reveal the standard quantum limit.

[1] Y. Y. Jiang, A. D. Ludlow, N. D. Lemke, R. W. Fox, J. a. Sherman, L. S. Ma, and C. W. Oates, Making optical atomic clocks more stable with 10^{-16} level laser stabilization, Nat. Photonics, **5**, 3 (2011).

[2] J. Lübbe, M. Temmen, S. Rode, P. Rahe, A. Kühnle, and M. Reichling, Thermal noise limit for ultra-high vacuum non-contact atomic force microscopy, Beilstein J. Nanotechnol. **4**, 32 (2013).

[3] T. Kessler, C. Hagemann, C. Grebing, T. Legero, U. Sterr, F. Riehle, M. J. Martin, L. Chen, and J. Ye, A sub-40-mHz-linewidth laser based on a silicon single-crystal optical cavity, Nat. Photonics **6**, 687 (2012).

[4] G. D. Cole, W. Zhang, M. J. Martin, J. Ye, and M. Aspelmeyer, Tenfold reduction of Brownian noise in high-reflectivity optical coatings, Nat. Photonics **7**, 644 (2013).

[5] T. P. Purdy, P. L. Yu, R. W. Peterson, N. S. Kampel, and C. A. Regal, Strong optomechanical squeezing of light, Phys. Rev. X **3**, 031012 (2013).

[6] LIGO Scientific Collaboration, Advanced LIGO, Classical Quantum Gravity **32**, 074001 (2015).

[7] VIRGO Collaboration, Virgo: A laser interferometer to detect gravitational waves, J. Instrum. **7**, P03012 (2012).

[8] KAGRA Collaboration, Interferometer design of the KAGRA gravitational wave detector, Phys. Rev. D **88**, 043007 (2013).

[9] K. Agatsuma, K. Arai, M.-K. Fujimoto, S. Kawamura, K. Kuroda, O. Miyakawa, S. Miyoki, M. Ohashi, T. Suzuki, R. Takahashi, D. Tatsumi, S. Telada, T. Uchiyama, and K. Yamamoto (CLIO Collaboration), Thermal-noise-limited underground interferometer CLIO, Classical Quantum Gravity **27**, 084022 (2010).

[10] A. V. Cumming, L. Cunningham, G. D. Hammond, K. Haughian, J. Hough, S. Kroker, I. W. Martin, R. Nawrodt, S. Rowan, C. Schwarz, and A. A. van Veggel, Silicon mirror suspensions for gravitational wave detectors, Classical Quantum Gravity **31**, 025017 (2014).

[11] G. D. Hammond, A. V. Cumming, J. Hough, R. Kumar, K. Tokmakov, S. Reid, and S. Rowan, Reducing the suspension thermal noise of advanced gravitational wave detectors, Classical Quantum Gravity **29**, 124009 (2012).

[12] F. Frasconi, Proceedings of the LVC Meeting, LOCATION, 2015 (unpublished).

[13] T. P. Purdy, R. W. Peterson, and C. A. Regal, Observation of radiation pressure shot noise on a macroscopic object, Science 339, 801 (2013).

[14] P. R. Saulson, Thermal noise in mechanical experiments, Phys. Rev. D 42, 2437 (1990).

[15] T. Corbitt, C. Wipf, T. Bodiya, D. Ottaway, D. Sigg, N. Smith, S. Whitcomb, and N. Mavalvala, Optical Dilution and Feedback Cooling of a Gram-Scale Oscillator to 6.9 mK, Phys. Rev. Lett. 99, 160801 (2007).

[16] C. M. Mow-Lowry, A. J. Mullavey, S. Goßler, M. B. Gray, and D. E. McClelland, Cooling of a Gram-Scale Cantilever Flexure to 70 mK with a Servo-Modified Optical Spring, Phys. Rev. Lett. 100, 010801 (2008).

[17] L. Ju, D. G. Blair, I. Bilenko, and D. Paget, Low loss niobium flexure suspension systems, Classical Quantum Gravity 19, 1703 (2002).

[18] M. Punturo et al., The Einstein Telescope: A third generation gravitational wave observatory, Classical Quantum Gravity 27, 010801 (2008).

[19] R. W. P. Drever, J. L. Hall, F. V. Kowalski, J. Hough, G. M. Ford, A. J. Munley, and H. Ward, Laser phase and frequency stabilisation using an optical resonator, Appl. Phys. B 31, 97 (1983).

[20] E. D. Black, A. Villar, K. Barbary, A. Bushmaker, J. Heefner, S. Kawamura, F. Kawazoe, L. Matone, S. Meidt, S. R. Rao, K. Schulz, M. Zhang, and K. G. Libbrecht, Direct observation of broadband coating thermal noise in a suspended interferometer, Phys. Lett. A 328, 1 (2004).

[21] K. Numata, M. Ando, K. Yamamoto, S. Otsuka, and K. Tsubono, Wide-Band Direct Measurement of Thermal Fluctuations in an Interferometer, Phys. Rev. Lett. 91, 260602 (2003).

[22] E. D. Black, A. Villar, and K. G. Libbrecht, Thermoelastic-Damping Noise from Sapphire Mirrors in a Fundamental-Noise-Limited Interferometer, Phys. Rev. Lett. 93, 241101 (2004).

[23] A. R. Neben, T. P. Bodiya, C. Wipf, E. Oelker, T. Corbitt, and N. Mavalvala, Structural thermal noise in gram-scale mirror oscillators, New J. Phys. 14, 115008 (2012).

[24] M. Kajima, N. Kusumi, S. Moriwaki, and N. Mio, Wide-band measurement of mechanical thermal noise using a laser interferometer, Phys. Lett. A 263, 21 (1999).

[25] K. Yamamoto, S. Otsuka, M. Ando, K. Kawabe, and K. Tsubono, Experimental study of thermal noise caused by an inhomogeneously distributed loss, Phys. Lett. A 280, 289 (2001).

[26] P. Paolino and L. Bellon, Frequency dependence of viscous and viscoelastic dissipation in coated micro-cantilevers from noise measurement, Nanotechnology 20, 405705 (2009).

[27] C. M. Mow-Lowry, Ph. D. thesis, Australian National University, 2011.

[28] L. Ju, D. G. Blair, M. Taniwaki, and R. Andrew, The quality factor of niobium flexure pendulums, Phys. Lett. A 254, 239 (1999).

[29] Piezomechanik HPSt 1000/25 − 15/5.

[30] E. D. Black, An introduction to Pound Drever Hall laser frequency stabilisation, Am. J. Phys. 69, 79 (2001).

[31] B. J. J. Slagmolen, Ph. D. thesis, Australian National University, 2004.

[32] V. B. Braginsky and S. P. Vyatchanin, Thermodynamical fluctuations in optical mirror coatings, Phys. Lett. A 312, 244 (2003).

[33] The PZT thermal noise is calculated using Eq. (1) with the following parameters: $Q = 70$, $\omega_0 = 2\pi \times 40$ kHz, $m = 11.5$ g.

[34] R. F. Greene and H. B. Callen, On a theorem of irreversible thermodynamics. II, Phys. Rev. 88, 1387 (1952).

[35] M. Cerdonio, L. Conti, A. Heidmann, and M. Pinard, Thermoelastic effects at low temperatures and quantum limits in displacement measurements, Phys. Rev. D 63, 082003 (2001).

[36] S. Rowan (private communication).